TRUE TIME DELAY BEAMSPACE WIDEBAND SOURCE LOCALIZATION

Nathan Wilkins, Arnab K. Shaw† & Majid Shaik†*

* Air Force Research Laboratory, Munitions Directorate, Eglin AFB, FL-32542, USA
†Electrical Engineering Department, Wright State University, Dayton, OH-45435, USA
Email: arnab.shaw@wright.edu

ABSTRACT

A novel method for signal subspace processing in the beamspace of a true time delay (TTD) beamformer bank is presented. The method permits the directions of arrival of broadband sources to be estimated accurately, efficiently and non-iteratively. This is achieved by exploiting the properties of the TTD beamformer bank, which simultaneously introduces spatial diversity into the data set while maintaining the broadband nature of the data. The beamspace manifold is derived and simulation results are presented. The method is shown to improve on the processing efficiency of previous broadband methods while maintaining source location estimation accuracy superior to conventional methods. It is also shown to resolve closely spaced and disparately spaced sources in a single algorithmic pass. The method is compared to previous method in terms of bias and RMSE.

Index Terms— Array signal processing, Direction-of-arrival (DOA) estimation, beamspace processing, Phased arrays, True time delay, Wideband, MUSIC

1. INTRODUCTION

This paper introduces a new method to perform source location processing at the output of a bank of TTD beamformers. Among the important work on wideband DOA estimation include the incoherent integration approach [1], the Coherent Signal Subspace (CSS) method that coherently transforms data in multiple frequency bins to a reference frequency that can then be processed by a narrowband method [2], [3], [4]. Performance of CSS depends on the accuracy of the preliminary estimates to be used as focusing angles and may require multiple iterations.

Frequency invariant beamforming for wideband direction finding in presented in [5] that uses reference beams. The data is transformed to frequency invariant beamspace to perform CSS processing [5] without requiring preliminary DOA estimates. Bilinear transform and dense array approximation was used in [5] to overcome the need for preliminary DOA estimates.

Gabriel had advocated the use of TTD beamforming to achieve wide bandwidth performance for high resolution large aperture sparse arrays [7]. A good overview of the TTD technology is given in [8]. Recent advances in RF Monolithic Microwave Integrated Circuit (MMIC) technology offer the promise of compact TTD beamforming architectures [9], [10]. Other developments include programmable architectures [11], [12], improvement in time delay resolution [13], and continuous variability [14].

Phase shifters used in conventional beamformers are frequency dependent and suffer from the beam squint phenomenon. TTD beamformers mitigate beam squint by preserving the pointing direction of the beamformers across multiple frequencies [15].

This paper extends MUSIC class of signal subspace array processing to beamspace processing at the output of TTD beamformer bank. The proposed method combines spatial diversity and beamspace processing, alleviating the need for preliminary AOA estimation. Improved bias and MSE performance is achieved at reduced computational expense. Unlike CSS, instantaneous source localization across the field of view is feasible, without requiring preliminary AOA estimation step or iterations to update AOA estimates. Also unlike CSS and similar frequency domain methods, it is primarily a time and spatial domain based technique.

2. PROBLEM FORMULATION

Fig. 1. depicts a sensor array and beamformer bank system. The sensor array is comprised of M Uniform Linear Array (ULA) antenna elements, where L far-field RF sources impinge on the array as planar wavefronts. For a K-beam bank, the kth beamformer output is given by,

$$y_k(t) = \sum_{m=1}^{M} w_m x_m(t - \tau_{m,k}^B(\theta_k^B)),\ k = 1,\cdots,K \tag{1}$$

where, $\tau_{m,k}^B(\theta_k^B) = \frac{d}{c}(m-1)\cos\theta_k^B$ is the TTD for the kth beamformer steered to beam direction θ_k^B at the mth sensor element. The weights w_m together with the TTD's define the beam pattern. $x_m(t)$ is the received response at the m^{th}

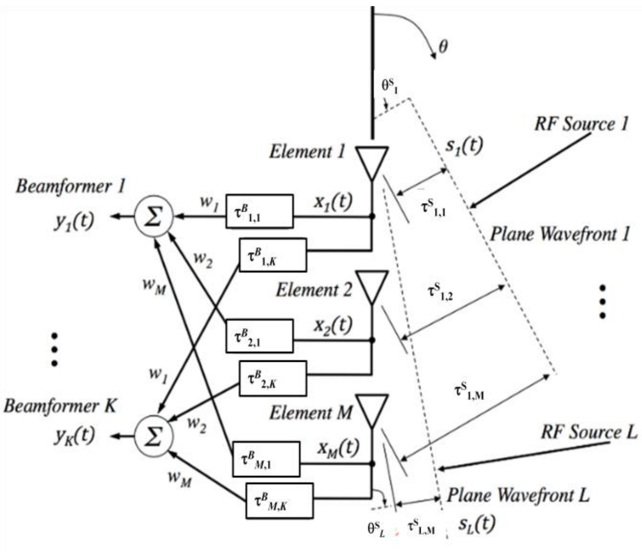

Fig. 1. Block diagram of element array and TTD beamformer bank system.

array element, and is the linear combination of the time delayed incident wavefront,

$$x_m(t) = \sum_{l=1}^{L} s_l(t - \tau_{l,m}^S(\theta_l^S)) + n_m(t);\ \ m = 1,\ldots M \tag{2}$$

where, θ_l^S is the Direction of Arrival (DOA) for the lth source, $s_l(t)$ denotes the l −th source, $n_m(t)$ is the noise at mth element. $\tau_{l,m}^S$ θ_l^S denotes the time delay for the l-th source at mth element, given by, $\tau_{l,m}^S(\theta_l^S) = \frac{d}{c}(m-1)\cos\theta_l^S$.

The wideband sources are modeled as,

$$s_l(t) = \sum_{j=1}^{J} \alpha_{j,l} e^{i2\pi f_j t}, l = 1, \ldots, L, \tag{3}$$

with spectral coefficients, $\alpha_{j,l}$, $j = 1, \ldots, J$. f_j is the center frequency of j-th sub-band. The kth beamformer response as given in (1) can be written as,

$$y_k(t) = \sum_{l=1}^{L}\sum_{m=1}^{M} w_m \sum_{j=1}^{J} \alpha_{j,l} e^{i2\pi f_j (t - \tau_{l,m}^s(\theta_l^s) - \tau_{m,k}^B(\theta_k^B))} + n_k(t), \tag{4}$$

$k = 1,\ldots,K$, where, $n_k(t)$ is the accumulated noise at each beamformer output. In matrix-vector form, the beamformer output snapshot $\boldsymbol{y}_K \triangleq [y_1(t) \cdots y_K(t)]^T$ can be written as,

$$\boldsymbol{y}_K = \sum_{j=1}^{J} e^{j2\pi f_j t} [\boldsymbol{\Phi}_{jB}(\boldsymbol{W}_{M\times L} \odot \boldsymbol{\Phi}_{js})]\boldsymbol{\alpha}_j + \boldsymbol{n}_K \tag{5}$$

where, the symbol "$\odot$" denotes the Hadamard product, $\boldsymbol{\alpha}_j \triangleq [\alpha_{j,1}\ \alpha_{j,2} \cdots \alpha_{j,L}]^T$,

$$[\boldsymbol{W}_{M\times L}]_{i,j} = w_j, \text{j}= 1, \ldots L \tag{6}$$

$$\{\boldsymbol{\Phi}_{jB}\}_{k,m} \in \mathbb{C}^{K\times M} = \left[e^{-i2\pi f_j \frac{d}{c}(m-1)\cos\theta_k^B}\right]_{k,m}; \quad k = 1,\ldots K, m = 0,\ldots, M-1 \tag{7}$$

$$\{\boldsymbol{\Phi}_{jS}\}_{m,l} \in \mathbb{C}^{M\times L} = \left[e^{-i2\pi f_j \frac{d}{c}(m-1)\cos\theta_l^B}\right]_{m,l}; \quad m = 0,\ldots, M-1, l = 1,\ldots, L \tag{8}$$

2.1 Manifold Derivation for a Single Source (L=1)

For a single source, *i.e.*, with $l = L = 1$, $\alpha_{j,l} = \alpha_j$, and the DOA being denoted as θ^s, the wideband signal model in equation (3) can be written as,

$$s_1(t) = \sum_{j=1}^{J} \alpha_j e^{i2\pi f_j t}. \tag{9}$$

From (8),

$$\phi_{js} \triangleq \boldsymbol{\Phi}_{js}\big|_{l=1} = \left[1 \quad e^{-i2\pi f_j \frac{d}{c}\cos\theta^s} \quad \cdots \quad e^{-i2\pi f_j \frac{d}{c}\ M-1\ \cos\theta^s}\right]^T \tag{10}$$

From equation (5) the jth frequency component of the beamspace manifold for $L = 1$ is given by,

$$\boldsymbol{\Phi}_{jB}\left(\boldsymbol{W}_{M\times 1} \odot \boldsymbol{\Phi}_{js}\big|_{l=1}\right) = \boldsymbol{\Phi}_{jB}(\boldsymbol{W}_{M\times 1} \odot \boldsymbol{\phi}_{js}) \qquad \in \mathbb{C}^{K\times 1}$$

$$= \begin{bmatrix} \sum_{m=1}^{M} w_m e^{-i2\pi f_j \frac{d}{c}(m-1)(\cos\theta_1^B + \cos\theta^S)} \\ \vdots \\ \sum_{m=1}^{M} w_m e^{-i2\pi f_j \frac{d}{c}(m-1)(\cos\theta_{B:K} + \cos\theta^S)} \end{bmatrix} \triangleq \boldsymbol{a}_B(f_j, \theta^S) \tag{11}$$

Using these in (5), it can be shown that the beamformer output vector with no noise is given by,

$$\boldsymbol{y}_K \triangleq A_B(\boldsymbol{f}, \theta^S)\, \boldsymbol{\alpha}_1 \tag{12}$$

where,

$$\boldsymbol{\alpha}_1 \triangleq \left[e^{i2\pi f_1 t}\alpha_1 \quad e^{i2\pi f_2 t}\alpha_2 \quad \cdots \quad e^{i2\pi f_J t}\alpha_J\right]^T \text{ and} \tag{13a}$$

$$A_B(\boldsymbol{f}, \theta^S) \triangleq \left[\boldsymbol{a}_B(f_1, \theta^S) \quad \cdots \quad \boldsymbol{a}_B(f_J, \theta^S)\right] \tag{13b}$$

where, $A_B(\boldsymbol{f}, \theta^S)$ represents the beam-space array manifold for a single source. The beamspace autocorrelation matrix for a single source is,

$$\mathbf{R}_B^{(1)} = E[\boldsymbol{y}_K \boldsymbol{y}_K^H] = \mathbf{A}_B(\boldsymbol{f}, \theta^S)\boldsymbol{\Lambda}_{\alpha_1}\mathbf{A}_B^H(\boldsymbol{f}, \theta^S) \tag{14}$$

where, $\boldsymbol{\Lambda}_{\alpha_1} \triangleq E[\boldsymbol{\alpha}_1\boldsymbol{\alpha}_1^H]$ is diagonal if the α_j's are uncorrelated. $\mathbf{R}_B^{(1)}$ has $\mathbf{R} = \mathbf{A}\boldsymbol{\Lambda}\mathbf{A}^H$ decomposition, but $A_B(\boldsymbol{f}, \theta^S)$ does not have typical Vandermonde structure. Also, the theoretical rank of $\mathbf{R}_B^{(1)}$ is not unity even if a single wideband source without any noise is present. However, it is important to note that the columns of $A_B(\boldsymbol{f}, \theta^S)$ within the signal bandwidth $B \in [f_1, f_J]$ define the signal subspace of $\boldsymbol{y}_K$, and $\boldsymbol{a}_B(f_j, \theta^S)$ defined in (11)-(12) represents the *spatio-spectral* beamspace steering vectors.

2.2. Multiple Wideband Sources

Assuming multiple uncorrelated sources having beamspace autocorrelation of the form in (14), the overall noiseless

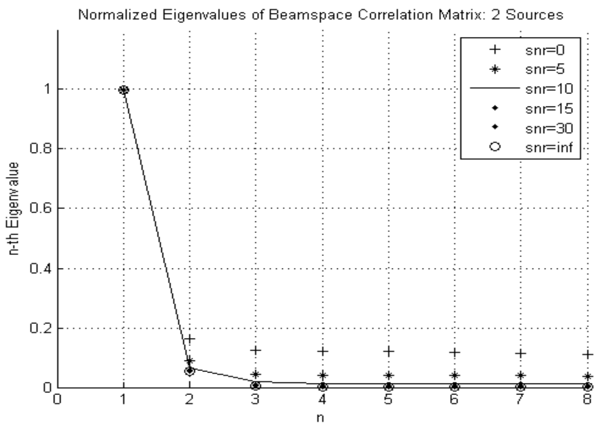

Fig. 2: Eigenvalues of beamspace correlation matrix, $L = 2$.

beamspace correlation matrix is given by [16, eqn.-(7)],

$$\mathbf{R}_B = \sum_{l=1}^{L} \mathbf{R}_B^{(l)} = \sum_{l=1}^{L} \mathbf{A}_B(\boldsymbol{f}, \theta_l^S)\mathbf{\Lambda}_{\alpha_l}\mathbf{A}_B^H(\boldsymbol{f}, \theta_l^S). \quad (15)$$

Assuming AWGN at each sensor,

$$\mathbf{R}_B = \sum_{l=1}^{L} \mathbf{R}_B^{(l)} + \sigma^2\mathbf{I}. \quad (16)$$

Clearly, $\mathbf{R} = \mathbf{A\Lambda A}^H$ type decomposition does not hold for multiple wideband sources. However, as evidenced by (15), the signal subspace information are contained in the column spaces of $\mathbf{A}_B(\boldsymbol{f}, \theta_l^S)$ for source angles θ_l over $B \in [f_1, f_J]$. Therefore, the beamspace steering vector in (11) is valid for multiple sources. It is important to note that the null-spaces of $\mathbf{R}_B$ are also the null spaces of individual $\mathbf{R}_B^{(l)}$'s [16]. Therefore, it is necessary to find the overall noise eigenvectors of $\hat{\mathbf{R}}_B$ only, and no need to find the eigenvectors of each $\mathbf{R}_B^{(l)}$ for individual sources.

2.3. Eigen-Analysis of Beamspace Correlation Matrix

The spatial beamspace correlation matrix is estimated as,

$$\hat{\mathbf{R}}_B = \mathbf{Y}_N\mathbf{Y}_N^H \in \mathbb{C}^{K\times K}. \quad (17)$$

where, $\mathbf{Y}_N = [\mathbf{y}_1 \cdots \mathbf{y}_N] \in \mathbb{C}^{K\times N}$. Figure 2 shows the distribution of normalized eigenvalues of $\hat{\mathbf{R}}_B$ for two sources at different SNR values. As expected, $\hat{\mathbf{R}}_B$ is full rank even with no noise (SNR=∞). However, the two (L=2) largest eigenvalues accounted for more than 99% energy for SNR $\geq$ 5dB, implying that L dominant eigenvectors retain significant signal subspace information. The weaker eigenvectors represent noise subspace, but may also contain small fraction of signal components. Accordingly, the orthogonality between $\boldsymbol{a}_B(f_j, \theta^S)$ and noise eigenvectors is only weakly valid, i.e.,

$$\boldsymbol{a}_B{}^H(f_j, \theta_l^S)\mathbf{v}_k \approx 0 \quad (18)$$

for $f_j \in B$, l = 1,..., L: k = L+1, ..., K. This work demonstrates that even with weak orthogonality, accurate wideband DOA estimation is feasible.

3. COMPUTATIONAL ALGORITHM

The approximate orthogonality of the steering vectors $\mathbf{a}_B(f_j, \theta^S)$ in (18) is utilized to define the proposed beamspace MUSIC-like spatial pseudo-spectra:

$$P_B(\theta) = \frac{1}{\frac{1}{J}\sum_{j=1}^{J}\frac{1}{M-L}\sum_{k=L+1}^{K}\left\| \boldsymbol{a}_B^H(f_j, \theta^S)\hat{\mathbf{v}}_k \right\|^2} \quad (19)$$

where, $\hat{\mathbf{v}}_k$'s are the eigenvectors corresponding to the smaller $K-L$ eigenvalues of $\hat{\mathbf{R}}_B$. The spectral footprint $B \in [f_1, f_J]$ of the sources and the number of sources present are assumed to be known. Notice that in (19), the summation is over signal bandwidth B, whereas, only the center frequency is used in narrowband MUSIC [17].

4. SIMULATION RESULTS

Consider a 16-element ULA of spacing $d = \lambda/2$,where λ is the wavelength of highest source frequency. For beamspace processing 8-beamformer bank was steered to [55° 65° 75° 85° 95° 105° 115° 125°]. The sources are wideband chirp waveforms of BW=400MHz and f_c=1 GHz. The Rayleigh resolution limit is 7.2° for M=16.

For the first experiment, two far-field chirp sources at 72° and 78° were simulated. For the 2nd experiment, an additional chirp source is at 108°. 4096 samples were collected for DOA processing. In case of CSS, the element space data are segmented into 64 blocks, and spectral covariance matrices were estimated at each FFT bin for focusing, etc.. For the proposed method a single beamspace correlation matrix was formed using (17) with the entire 4096 snapshots. The dashed vertical lines indicate the true DOA values in all figures. For CSS, an initial estimate of 76° was used to form the diagonal focusing matrices (see eq. (29) of [2]) and one iteration was used in both simulations. The proposed method does not require initial estimates, and the summation in (11) was evaluated over $f_c \pm 30$MHz at 1MHz interval. The performance of both methods are comparable for 2 sources (Fig. 3). For the 3-source case, the proposed method estimates all 3 DOAs correctly in a single pass (Fig. 4). In case of CSS, one of the sources is biased, and would require another pass of CSS with a new DOA estimate in the direction of the third DOA.

4.1. Computation Cost Comparison

The proposed TTD-based approach does not transform the data to the frequency domain and processes one $K\times K$ beamspace correlation matrix in (17), as opposed to multiple $M\times M$ spectral correlation matrices used by CSS [2], [3]. The overall computation cost analysis has been provided in

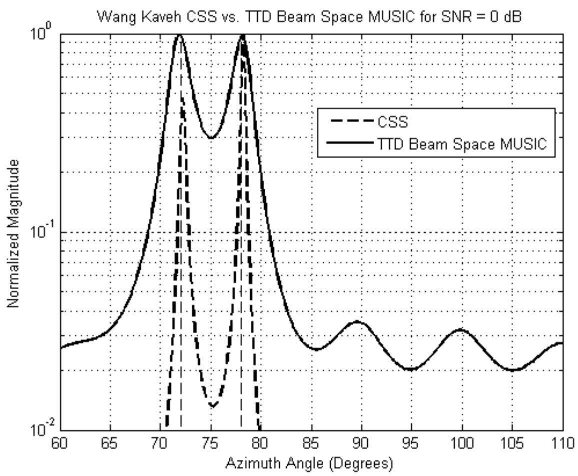

Fig. 3: Performance comparison for 2 Chirp sources at 0dB.

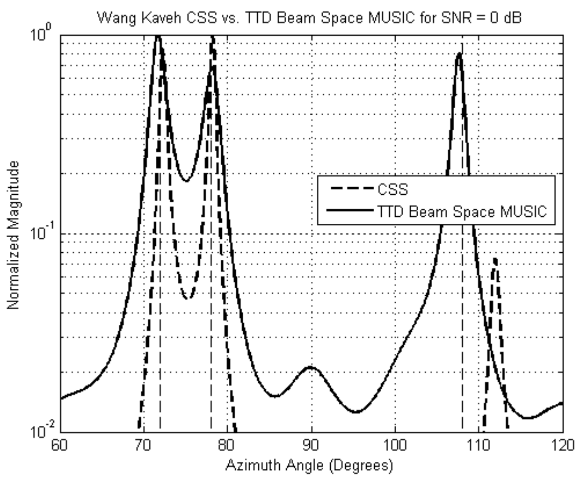

Fig. 4: Performance comparison for 3 Chirp sources at 0dB.

[18] where it is shown that the operations count for the TTD approach is $\xi_{TTD} = O(K^2N + K^3)$. Fig. 5 shows the theoretical and calculated computational expense vs. N, the data sequence lengths for 1000 runs for each method. The calculations assume M=16, CSS parameters from [2], [3] and K=8 for TTD signal subspace processing.

4.2. Estimation Bias and RMSE Comparison

The bias and RMSE with 100 independent runs are shown in Fig. 6 and Fig. 7, for one of the DOAs, which show consistent performance over a broad range of SNR values.

5. CONCLUSION

This paper presents a novel method of signal subspace processing in the beam space of a true time delay beamformer bank. The proposed algorithm models the wideband data in terms of component frequencies [see (3)], which enables evaluating the MUSIC-like pseudo-spectrum [see (19)] by searching over arbitrary number of frequencies within the source bandwidth. The method

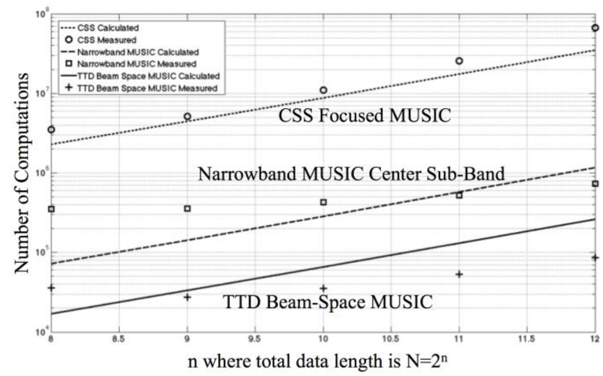

Fig. 5. Computational complexity comparison

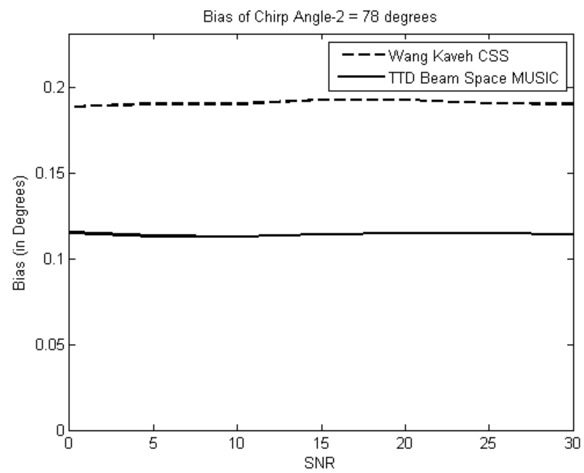

Fig. 6: Bias for DOA=78° over 100 independent runs.

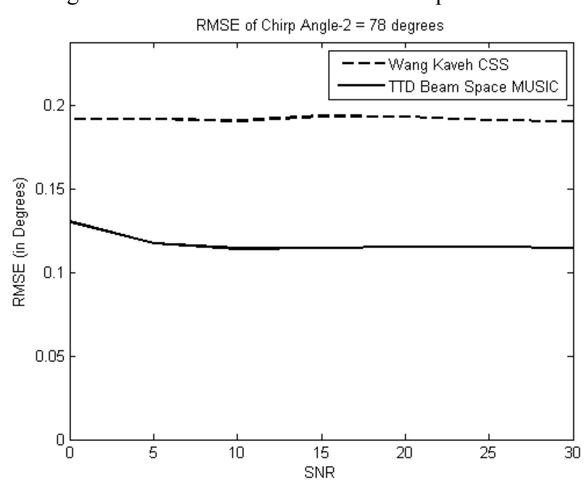

Fig. 7: RMSE for DOA=78° over 100 independent runs.

performs high-resolution wide bandwidth RF source location estimation that does not require preliminary DOA estimates. It performs the processing in a single pass of the algorithm for the entire field of view, and is capable of achieving significant savings in computational expense as compared to previous methods for cases when the number of beamformers in the true time delay beamformer bank is less than the number of array elements.

5. REFERENCES

[1] M. Wax and T. Kailath, "Detection of Signals by Information Theoretic Criteria," *IEEE Transactions on Acoustics, Speech and Signal Processing*, Vol. ASSP-33, No. 2, pp. 387-392,April 1985.

[2] H. Wang and M. Kaveh, "Coherent Signal-Subspace Processing for the Detection and Estimation of Angles of Arrival of Multiple Wide-Band Sources," *IEEE Transactions on Acoustics, Speech and Signal Processing*," Vol. ASSP-33, No. 4, pp. 823-831, August 1985.

[3] H. Wang and M. Kaveh, "On the Performance of Signal-Subspace Processing – Part II: Coherent Wide-Band Systems," *IEEE Transactions on Acoustics, Speech and Signal Processing*, Vol. ASSP-35, No. 11, pp. 1583-1591, November 1987.

[4] H. Hung and M. Kaveh, "Focusing Matrices for Coherent Signal-Subspace Processing," *IEEE Transactions on Acoustics, Speech and Signal Processing*, Vol. 36, pp. 1272-1281, August 1988.

[5] A. Shaw and R. Kumaresan, "Estimation of Angles of Arrival of Broadband Sources," *Proceedings of the IEEE International Conference on Acoustics, Speech and Signal Processing*, pp. 2296-2299, April 1987.

[6] T. Lee, "Efficient Wideband Source Localization Using Beamforming Invariance Technique," *IEEE Transactions on Signal Processing*," Vol. 42, No. 6, pp. 1376-1387, June 1994.

[7] W. F. Gabriel, "Large-Aperture Sparse Array Antenna Systems of Moderate Bandwidth for Multiple Emitter Location," *IEEE Transactions on Antennas and Propagation*, Vol. 37, No. 1, pp. 16-29, January 1989.

[8] L. H. Gesell, T. M. Turpin and M. W. Rubin, "True Time Delay Beamforming Using Fiber Optic Cavities," *SPIE,* Vol. 2560, pp. 130-139, 1995.

[9] M. Longbrake, J. Buck, P. Buxa, T. Dalrymple, J. McCann, R. Neidhard, P. Watson, K. Zeller, B. Garber and D. Kuhl, "TELA Testbed Time Delay Beam Steering Demonstration," *Proceedings of the Antenna Measurement Techniques Association*, pp. 185-190, 2009.

[10] B. Thompson, "True Time Delay Module Finds Needle in a Haystack Frequencies," Wright-Patterson Air Force Base online press release, Available at http://www.wpafb.af.mil/news, Wright-Patterson Air Force Base, 2011.

[11] R. Mucci, "A Comparison of Efficient Beamforming Algorithms," *IEEE Transactions on Acoustics, Speech and Signal Processing*, Vol. ASSP-32, No. 3, pp. 548-558, 1984.

[12] X. Zheng, N. Kim and A. Siahmakoun, "High-speed programmable true-time-delay optical beamformer based on recirculating loop," *Proceedings of the Optical Fiber Communication Conference*, Optical Society of America, Los Angeles, CA, vol. 2,February 2004.

[13] J. Roderick, H. Krishnaswamy, K. Newton and H. Hashemi, "A 4-bit Ultra-Wideband Beamformer with 4ps True Time Delay Resolution," *Proceedings IEEE Custom Integrated Circuit Conference*, San Jose CA, pp. 805-808,2005.

[14] D. Hunter, M. Parker and J. Dexter, "Demonstration of a Continuously Variable True-Time Delay Beamformer Using a Multichannel Chirped Fiber Grating," *IEEE Transactions on Microwave Theory and Techniques*, Vol. 54, No. 2, pp. 861-867, February 2006.

[15] M. Longbrake, "True Time-Delay Beamsteering for Radar," Proceedings *of the IEEE National Aerospace and Electronics Conference (NAECON '12)*, pp. 246–249, 2012.

[16] R. O. Schmidt, "Multiple Emitter Location and Signal Parameter Estimation," *IEEE Transactions on Antennas and Propagation*, Vol. 34, No. 3, pp. 276-280,March 1986.

[17] M. Agrawal and S. Prasad, "Broadband DOA Estimation Using "Spatial-Only" Modeling of Array Data," *IEEE Transactions on Signal Processing*, Vol. 48, No. 3, pp. 663 - 670, Mar 2000.

[18] N. Wilkins, *Signal Subspace Processing in the Beam Space of a True Time Delay Beamformer Bank*, Ph.D. Dissertation, Wright State University, Dayton, OH, May, 2015.